The Eurasia Proceedings of Science, Technology, Engineering & Mathematics (EPSTEM)
ISSN: 2602-3199

The Eurasia Proceedings of Science, Technology, Engineering and Mathematics (EPSTEM), 2025

Volume 38, Pages 56-68

IConTES 2025: International Conference on Technology, Engineering and Science

Robust Nonlinear Control of a 3×2 Stacked Multicellular Inverter Using Neural Network-Based Regulation

Salah Hanafi
Djillali Liabes University of Sidi Bel-Abbes

Mohammed Karim Fellah
Djillali Liabes University of Sidi Bel-Abbes

Youcef Djeriri
Djillali Liabes University of Sidi Bel-Abbes

Mohamed Fouad Benkhoris
University of Nantes

Abdelhakim Saim
University of Nantes

Djamel Ziane
University of Nantes

Patrice Wira
University of Haute Alsace

Abstract: The increasing demand for high-performance power converters has led to the development of advanced control strategies that enhance system robustness against load variations. This paper presents a novel control approach for a 3×2 stacked multicellular inverter, integrating nonlinear feedback decoupling control with neural network - based regulators. Unlike conventional Proportional-Integral (PI) controllers, which struggle with parameter variations and dynamic uncertainties, the proposed neural network (NN) controller adapts in real-time to maintain system stability and optimal performance. The NN is trained to approximate the nonlinear control law while compensating for parametric variations and external disturbances. A comparative analysis between the NN-based control and the traditional PI approach is conducted using MATLAB / Simulink simulations, evaluating response time, harmonic distortion (THD), and robustness against load changes. The results demonstrate that the NN-based controller significantly improves system adaptability, robustness and voltage regulation, making it a promising solution for modern power conversion systems.

Keywords: Stacked multicellular inverter, Nonlinear feedback decoupling control, Neural network, Robust control

Introduction

The growing demand for efficient and reliable power conversion systems, driven by the rapid expansion of renewable energy integration, electric mobility, and advanced industrial drives, has placed multilevel converter topologies at the forefront of modern power electronics research (Akagi, 2017; Blaabjerg et al., 2013). Among them, the multicellular converters, where they are divided into three types namely the series, stacked and parallel

- This is an Open Access article distributed under the terms of the Creative Commons Attribution-Noncommercial 4.0 Unported License, permitting all non-commercial use, distribution, and reproduction in any medium, provided the original work is properly cited.

- Selection and peer-review under responsibility of the Organizing Committee of the Conference

© 2025 Published by ISRES Publishing: www.isres.org

multicellular converters. The stacked multicellular converter (SMC) architecture has emerged as a promising solution due to its modularity, improved voltage quality, and enhanced fault tolerance (Meynard et al., 2002; Rodriguez et al., 2009). By generating multilevel voltage waveforms, SMCs achieve lower harmonic distortion and higher power quality, which makes them particularly attractive for applications such as smart grids, renewable energy systems, and high-performance motor drives (Kouro et al., 2010; Wu, 2006).

Nevertheless, the control of multicellular converters topologies remains a challenging task because of their nonlinear dynamics, strong inter-cell couplings, and sensitivity to load and parameter variations (Bakeer et al., 2022). Traditional control strategies, particularly Proportional–Integral (PI) regulators, remain widely adopted in industrial practice due to their simple structure and ease of implementation. However, their effectiveness is severely limited under dynamic uncertainties and varying operating conditions, often resulting in degraded performance and instability (Peña-Alzola et al., 2014). These challenges have stimulated the development of advanced control strategies capable of ensuring robustness, adaptability, and superior dynamic performance (Hanafi et al., 2016, 2021).

In this context, nonlinear feedback decoupling control has been shown by Gateau et al. (1997) to be an effective approach for handling the coupling phenomena and complex dynamics inherent in flying multicellular converters. Building on this principle, Hanafi et al. have demonstrated the successful application of nonlinear feedback decoupling technique to control the stacked multicellular converter, achieving improved voltage regulation and enhanced stability in Hanafi et al. (2014). More recently, neural network (NN)-based approaches have been introduced to further enhance the control of multicellular converters, particularly in modulation strategies, where they have proven effective in improving robustness and adaptability (Hanafi et al., 2025).

Artificial intelligence (AI)-driven control methods, and neural networks in particular, offer several advantages in power electronics. Their universal approximation capability and adaptive learning nature allow them to capture complex nonlinear dynamics and compensate for parametric uncertainties (Isidori, 1995; Haykin, 2009). Consequently, NN-based regulators have been successfully applied to multilevel converters for predictive control (Bakeer et al., 2022; Rivera et al., 2013) and adaptive regulation in renewable energy systems (Jiang et al., 2021). Despite these advances, limited research has addressed the combination of nonlinear feedback decoupling and neural network-based regulation in stacked multicellular converters, leaving open opportunities for performance enhancement in robustness, dynamic response, and power quality.

To address this gap, this paper proposes a novel control scheme that integrates nonlinear feedback decoupling with neural network-based regulators for a 3×2 SMC converter. The proposed method leverages the strengths of nonlinear decoupling while exploiting the adaptive learning capabilities of NNs to ensure stable operation under parametric variations, load disturbances, and dynamic uncertainties. A comparative analysis with conventional PI controllers is performed using MATLAB/Simulink simulations, with evaluation metrics including transient response, total harmonic distortion (THD), and robustness to load variations. The results confirm that the NN-based decoupling strategy provides superior adaptability, improved voltage regulation, and enhanced power quality, positioning it as a promising candidate for next-generation power conversion systems.

Stacked Multicellular Converter

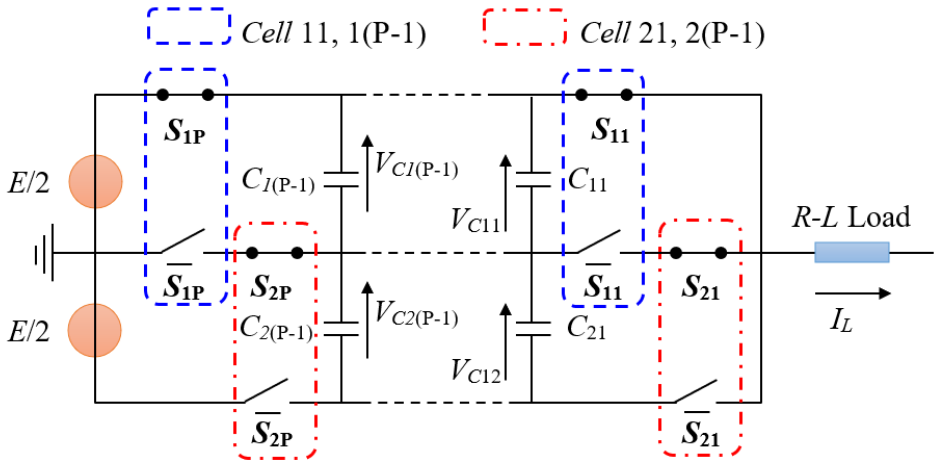

Figure 1. A stacked multicellular converter $P \times 2$ powering an R-L load.

The stacked multicellular converter (SMC), first introduced in the early 2000s, is composed of n stacks, each formed by a series connection of P switching cells separated by $(P-1)$ floating capacitors. The SMC converter consists of a hybrid association of commutation cells (Figure 1). In the case of $(P \times 2)$ configuration, the structure consists of P columns and $(n = 2)$ stacks, resulting in $(P \times n)$ commutation cells and $((P-1) \times n)$ floating capacitors (Lienhardt et al., 2005). Such a topology is capable of generating $((P \times 2) + 1)$ voltage level. The upper stack operates exclusively during positive output cycles, while the lower stack is activated during negative output cycles. The modeling of the average behavior of a stacked multicellular converter relies on the following assumptions:

- The switches are considered ideal, i.e., with zero saturation voltage, no leakage current, and negligible dead time or switching delay.
- The two switches within the same commutation cell operate in a complementary manner.
- The values of the floating capacitors C_{i1} and C_{2i} are such that the voltages at their terminals, $V_{C_{i1}}$ and $V_{C_{i2}}$ are constants over a cutting period.
- The load current I_L is constant over a cutting period and corresponds to the average value of this one over the same period.
- The DC supply voltage E is constant.

Under these assumptions, Equation (1) describes the dynamics of the floating capacitor voltages $\left(V_{C_{i1}}, V_{C_{i2}}\right)$ in the two stacks, as well as the evolution of the load current I_L, when the stacked multicellular converter operates as an inverter supplying an R-L load:

$$\begin{cases} \frac{d}{dt}V_{C_{11}} = \frac{S_{12}-S_{11}}{C_{11}} \cdot I_L \\ \frac{d}{dt}V_{C_{12}} = \frac{S_{13}-S_{12}}{C_{12}} \cdot I_L \\ \frac{d}{dt}V_{C_{21}} = \frac{S_{22}-S_{21}}{C_{21}} \cdot I_L \\ \frac{d}{dt}V_{C_{22}} = \frac{S_{23}-S_{22}}{C_{22}} \cdot I_L \\ \frac{d}{dt}I_L = -\frac{R_L}{L_L}I_L + \frac{S_{11}-S_{12}}{L_L}V_{C_{11}} + \frac{S_{12}-S_{13}}{L_L}V_{C_{12}} + \frac{S_{21}-S_{22}}{L_L}V_{C_{21}} + \frac{S_{22}-S_{23}}{L_L}V_{C_{22}} + \frac{S_{13}E_1}{L_L} + \frac{(S_{23}-1)E_2}{L_L} \end{cases} \quad (1)$$

Based on equation (1), it is possible to establish the state equation of the system:

$$\dot{X} = A \cdot X + B(X) \cdot U \quad (2)$$

The mathematical representation of the 3×2 SMC is given as follows:

$$X = [V_{C_{11}} \quad V_{C_{12}} \quad I_L \quad V_{C_{21}} \quad V_{C_{22}} \quad I_L]^T$$
$$U = [S_{11} \quad S_{12} \quad S_{13} \quad S_{21} \quad S_{22} \quad S_{23}]^T$$

$$B(X) = \begin{pmatrix} -\frac{I_L}{C_{11}} & \frac{I_L}{C_{11}} & 0 & 0 & 0 & 0 \\ 0 & -\frac{I_L}{C_{12}} & \frac{I_L}{C_{12}} & 0 & 0 & 0 \\ \frac{V_{C_{11}}}{L_L} & \frac{V_{C_{12}}-V_{C_{11}}}{L_L} & \frac{E_1-V_{C_{12}}}{L_L} & \frac{V_{C_{21}}}{L_L} & \frac{V_{C_{22}}-V_{C_{21}}}{L_L} & \frac{E_2-V_{C_{22}}}{L_L} \\ 0 & 0 & 0 & -\frac{I_L}{C_{21}} & \frac{I_L}{C_{21}} & 0 \\ 0 & 0 & 0 & 0 & -\frac{I_L}{C_{22}} & \frac{I_L}{C_{22}} \\ \frac{V_{C_{11}}}{L_L} & \frac{V_{C_{12}}-V_{C_{11}}}{L_L} & \frac{E_1-V_{C_{12}}}{L_L} & \frac{V_{C_{21}}}{L_L} & \frac{V_{C_{22}}-V_{C_{21}}}{L_L} & \frac{E_2-V_{C_{22}}}{L_L} \end{pmatrix}$$

$$A = \begin{pmatrix} 0 & 0 & 0 & 0 & 0 & 0 \\ 0 & 0 & 0 & 0 & 0 & 0 \\ 0 & 0 & -\frac{R_L}{L_L} - \frac{E_2}{L_L \cdot I_L} & 0 & 0 & 0 \\ 0 & 0 & 0 & 0 & 0 & 0 \\ 0 & 0 & 0 & 0 & 0 & 0 \\ 0 & 0 & 0 & 0 & 0 & -\frac{R_L}{L_L} - \frac{E_2}{L_L \cdot I_L} \end{pmatrix}$$

The load current is duplicated in the state vector X in order to obtain a square matrix $B(X)$ of dimension 6×6, which makes it possible to compute its inverse for use in the subsequent control design. Since the vector X explicitly appears in the expression of $B(X)$ in matrix equation (2), the system exhibits nonlinear behavior. In addition, $B(X)$ is not a diagonal matrix: each input component (S_{1i}, S_{2i}) simultaneously affects multiple state variables, and conversely, each state variable depends on several input components. Consequently, the system can be characterized as strongly coupled (Gateau et al., 2002).

Hybrid Nonlinear Feedback Decoupling Control with Neural Network Regulators

Nonlinear Feedback Decoupling Control

Nonlinear feedback decoupling control enables the decoupling between system inputs and outputs while ensuring the stabilization of the floating capacitor voltages. From the model described in equation (2), it is possible to define a column matrix $\alpha(X)$ and a square matrix $\beta(X)$ such that, by selecting the control input as $U(X) = \alpha(X) + \beta(X).V$, the closed-loop system exhibits linear behavior with complete decoupling between inputs and outputs (Aimé, 2003). From the matrix system:

$$\begin{cases} \dot{X} = A \cdot X + B(X) \cdot U \\ U = \alpha(X) + \beta(X) \cdot V \end{cases}$$

By substituting the expression of U, we obtain:

$$\dot{X} = A \cdot X + B(X) \cdot \alpha(X) + B(X) \cdot \beta(X) \cdot V \tag{3}$$

The matrix $\alpha(X)$ is defined in such a way that the product $(B(X).\alpha(X))$ fully compensates the term $(A.X)$. In addition, the matrix $B(X)$ remains invertible under the condition that:

$$I_L \neq 0 \quad \text{and} \quad E \neq 0 \tag{4}$$

Consequently, we choose:

$$\beta(X) = B^{-1}(X) \tag{5}$$

Let:

$$\dot{V}_{C_{11}} = v_{11}, \quad \dot{V}_{C_{12}} = v_{12}, \quad \dot{I}_L = v_{13}, \quad \dot{V}_{C_{22}} = v_{22}, \quad \dot{V}_{C_{22}} = v_{22}, \quad \dot{I}_L = v_{23} \tag{6}$$

The matrixes $\alpha(X)$ and $\beta(X)$ are given as:

$$\alpha(X) = -B^{-1}(X).A.X$$

$$\beta(X) = B^{-1}(X)$$

According to the conditions defined in (4), the results of the decoupling computation are expressed in (7).

$$A \cdot X = (0 \quad 0 \quad -b_0 X_{13} - b_1 E_2 \quad 0 \quad 0 \quad -b_0 X_{13} - b_1 E_2)^T \tag{7}$$

$$B^{-1}(X) = \begin{pmatrix} \frac{X_{11}-E_1}{a_{11}E_1X_{13}} & \frac{X_{12}-E_1}{a_{12}E_1X_{31}} & \frac{1}{2b_1E_1} & 0 & 0 & \frac{1}{2b_1E_1} \\ \frac{X_{11}}{a_{11}E_1X_{13}} & \frac{X_{12}-E_1}{a_{12}E_1X_{13}} & \frac{1}{2b_1E_1} & 0 & 0 & \frac{1}{2b_1E_1} \\ \frac{X_{11}}{a_{11}E_1X_{13}} & \frac{X_{12}}{a_{12}E_1X_{13}} & \frac{1}{2b_1E_1} & 0 & 0 & \frac{1}{2b_1E_1} \\ 0 & 0 & \frac{1}{2b_1E_1} & \frac{X_{21}-E_2}{a_{21}E_2X_{32}} & \frac{X_{22}-E_2}{a_{22}E_2X_{32}} & \frac{1}{2b_1E_1} \\ 0 & 0 & \frac{1}{2b_1E_1} & \frac{X_{21}}{a_{21}E_2X_{32}} & \frac{X_{22}-E_2}{a_{22}E_2X_{32}} & \frac{1}{2b_1E_1} \\ 0 & 0 & \frac{1}{2b_1E_1} & \frac{X_{21}}{a_{21}E_2X_{32}} & \frac{X_{22}}{a_{22}E_2X_{32}} & \frac{1}{2b_1E_1} \end{pmatrix} \quad (8)$$

with:

$$a_{11} = \frac{1}{C_{11}}, a_{12} = \frac{1}{C_{12}}, a_{21} = \frac{1}{C_{21}}, a_{22} = \frac{1}{C_{22}}, b_0 = \frac{R_L}{L_L}, b_1 = \frac{1}{L_L}$$

Consequently, the feedback control law is formulated as:

$$\alpha(X) = \left(\frac{b_0X_{13}+b_1E_2}{b_1E_1} \quad \frac{b_0X_{13}+b_1E_2}{b_1E_1} \quad \frac{b_0X_{13}+b_1E_2}{b_1E_1} \quad \frac{b_0X_{13}+b_1E_2}{b_1E_1} \quad \frac{b_0X_{13}+b_1E_2}{b_1E_1} \quad \frac{b_0X_{13}+b_1E_2}{b_1E_1}\right)^T \quad (9)$$

Once the state feedback is implemented, the resulting input variables are represented by the vector $V = (v_{11} \quad v_{12} \quad v_{13} \quad v_{21} \quad v_{22} \quad v_{23})^T$ (Figure 2).

For a stacked multicellular converter, the application of nonlinear feedback makes it possible to derive $P \times 2$ linear relations, ensuring complete decoupling between the new input variables and the $P \times 2$ state system variables.

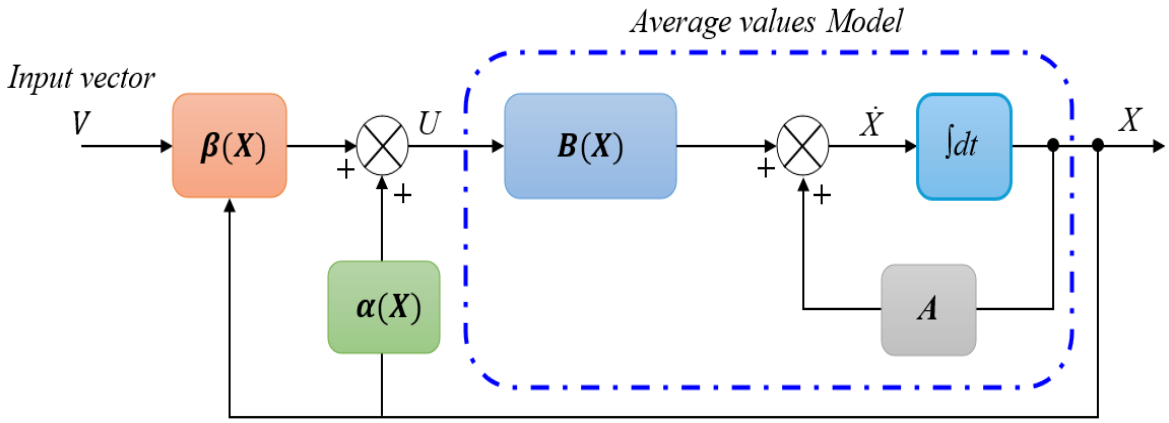

Figure 2. Decoupling with nonlinear feedback: functional representation.

A singularity arises in the vicinity where nonlinear decoupling control loses its validity. These singular points correspond to the zero crossing of the load current ($I_L = 0$) and the DC supply voltage ($E = 0$). Under such conditions, the system becomes uncontrollable (Gateau, 1997; Gateau et al., 1997). In the case of a chopper, these singularities have no impact since they fall outside the normal operating range. Conversely, for an SMC inverter, the load current reaches zero twice during each fundamental period. Therefore, it is necessary to introduce a limitation on the measured current in order to avoid the singular point at ($I_L = 0$) as illustrated in Figure 3.

After decoupling the different variables, the system is transformed into $P \times 2$ linear subsystems, where each subsystem links an input variable to a state variable $(\dot{X} = V)$. It then becomes necessary to introduce a second linear control loop to impose the desired dynamics on each state variable. As illustrated in Figure 3, this requires as many feedback loops as there are state variables.

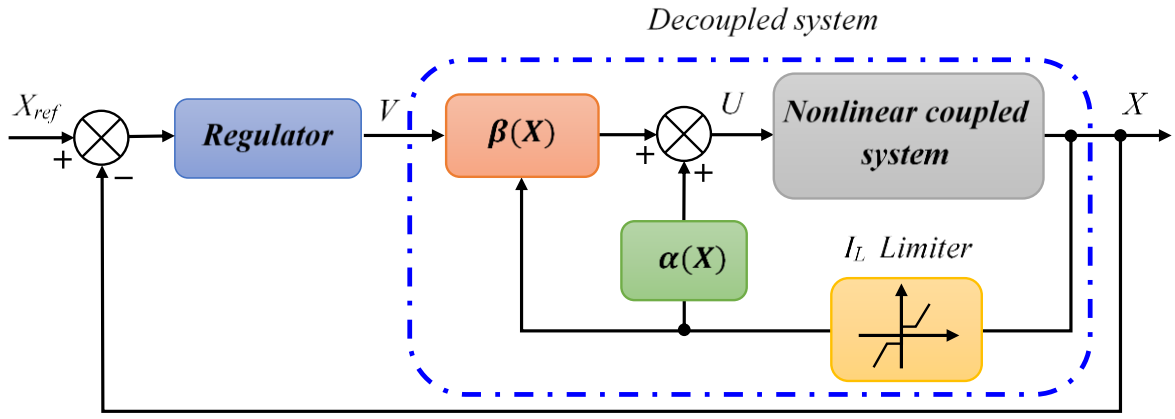

Figure 3. Enslavement of the decoupled system to a reference vector X_{ref}.

Neural Network Regulators

To overcome the limitations of classical PI regulators in nonlinear decoupling control, this work proposes a hybrid approach that integrates a nonlinear feedback decoupling law with neural network (NN)-based regulators (Figure 4). The nonlinear feedback structure ensures the separation of the control dynamics between load current and floating capacitor voltages, thereby reducing cross-coupling effects and enhancing stability. However, the performance of the conventional PI regulators, when embedded in this framework, is often limited under varying operating conditions due to their inability to adapt online.

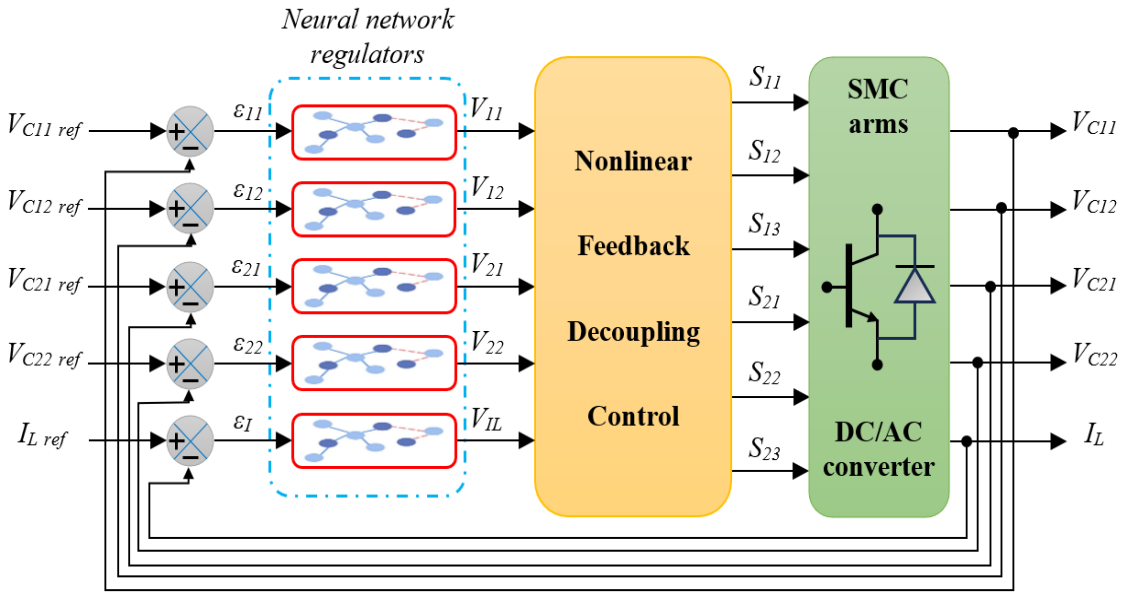

Figure 4. Block diagram of the designed hybrid nonlinear feedback decoupling control with neural network regulators.

In the proposed hybrid strategy, Proportional–Integral regulators are replaced with feed-forward multilayer perceptron (MLP) neural networks. Each NN is trained offline using data generated from the nominal PI controllers and then fine-tuned online to account for parametric variations and external disturbances. The general mathematical structure of the NN regulator can be expressed as:

$$Y_j^l = f\left(\sum_t^{nl} W_{ji}^l X_i + b_j^l\right) \tag{10}$$

where,

X_i: inputs vector,
W_{ji}^l: synaptic weights of neuron j in layer l,
b_j^l: bias input,
f: activation function (sigmoidal transfer function).

The architecture adopted in this work consists of a static feed-forward MLP with an input layer representing the error signals, one hidden layer with ten neurons using a sigmoid activation function, and one output neuron providing the reference control voltage. The training parameters include a learning rate of 1×10^6, momentum coefficient of 4.49×10^3, and a maximum of 1000 epochs. The network was validated using mean squared error (MSE) criteria, ensuring convergence without overfitting.

By embedding the neural network regulators inside the nonlinear feedback decoupling scheme, the system benefits from both the structural robustness of decoupling control and the adaptive learning capability of neural networks. Simulation results demonstrate that this hybrid strategy achieves improved current tracking, reduced harmonic distortion (THD), and better stabilization of floating capacitor voltages compared to the conventional PI-based decoupling approach.

Results and Discussions

This section presents the simulation results and discussion for a 3×2 stacked multicellular DC/AC converter controlled by the nonlinear feedback decoupling strategy. The performance of the proposed hybrid scheme, which integrates neural network (NN)-based regulators into the nonlinear decoupling law, is compared against the classical PI-based approach to evaluate accuracy, robustness, and adaptability. Simulations were performed in MATLAB/Simulink using the following parameters (Table 1):

Table 1. Parameters used in simulations

Parameters	Numerical values
P (Cells number)	3
n (Stack number)	2
E (DC voltage)	1500 V
C (Floating capacitor)	400 μF
L_L (Load inductance)	0.1 mH
R_L (Load resistance)	10 Ω
f_c (Cutting frequency)	28 KHz
K_{pV_c}	30000
K_{iV_c}	10
K_{pI_L}	2000000
K_{iI_L}	10

These values provide a realistic operating framework and enable the assessment of system behavior under different disturbances and operating conditions. To comprehensively evaluate the controllers, three scenarios were considered:

1. Reference load current regulation: This scenario tests the ability of the controllers to accurately track step variations in the reference load current. The objective is twofold: to verify the current regulation capability of the system, and to analyze whether current variations remain decoupled from the capacitor voltages.
2. Variation of DC input voltage: In this scenario, the input DC source is perturbed to examine the stability and dynamic response of the system. Again, the goal is twofold: to ensure that the floating capacitor voltages are well regulated despite input voltage fluctuations, and to highlight the decoupling between input voltage dynamics and load current regulation.
3. Load parameter variations: The third scenario evaluates the robustness of the controllers under changes in load resistance and inductance. This test assesses the adaptability of both PI- and NN-based regulators when subjected to parametric uncertainties, ensuring reliable operation under realistic load disturbances.

The comparative results under these three conditions demonstrate that both control schemes achieve satisfactory performance; However, the NN-based regulators offer noticeable advantages in terms of faster transient response, improved decoupling behavior, and enhanced robustness to load variations.

Floating Capacitor Voltage Regulation

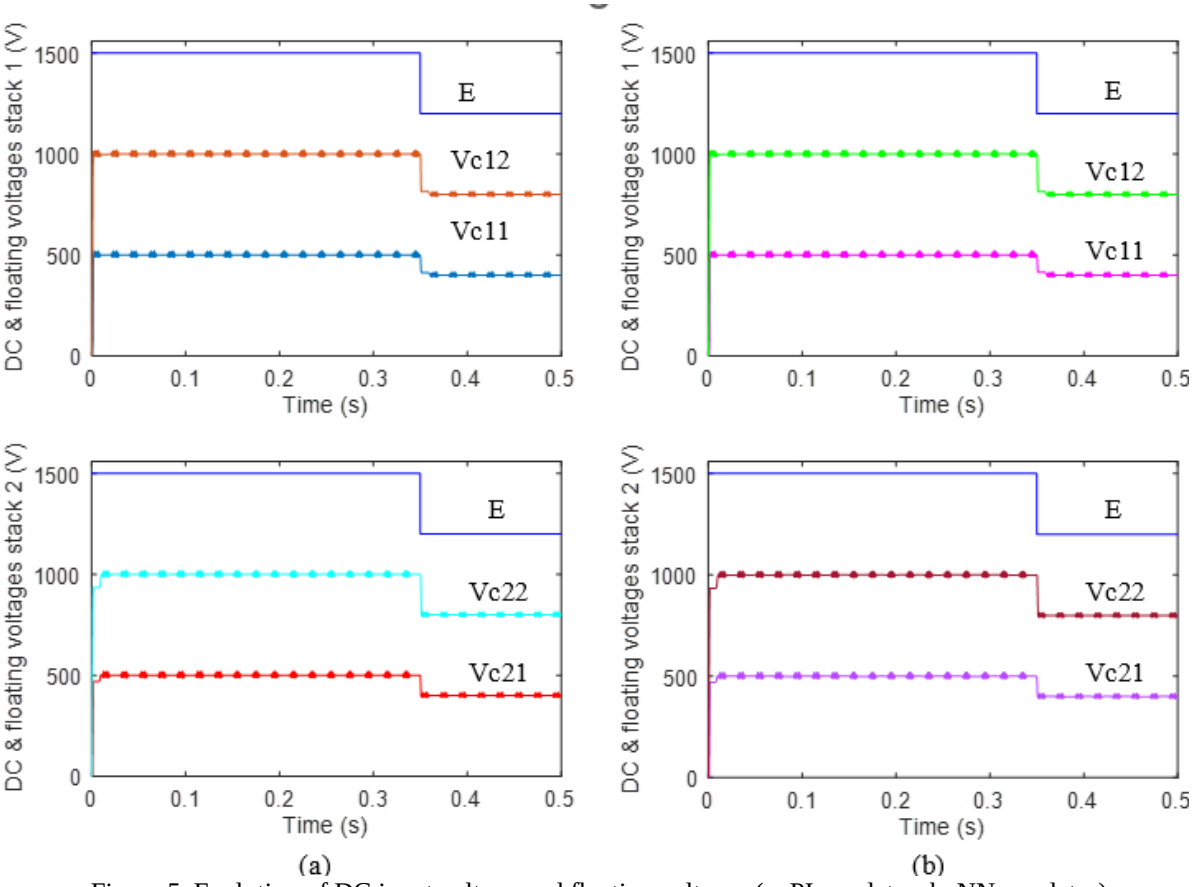

Figure 5. Evolution of DC input voltage and floating voltages (a: PI regulator, b: NN regulator)

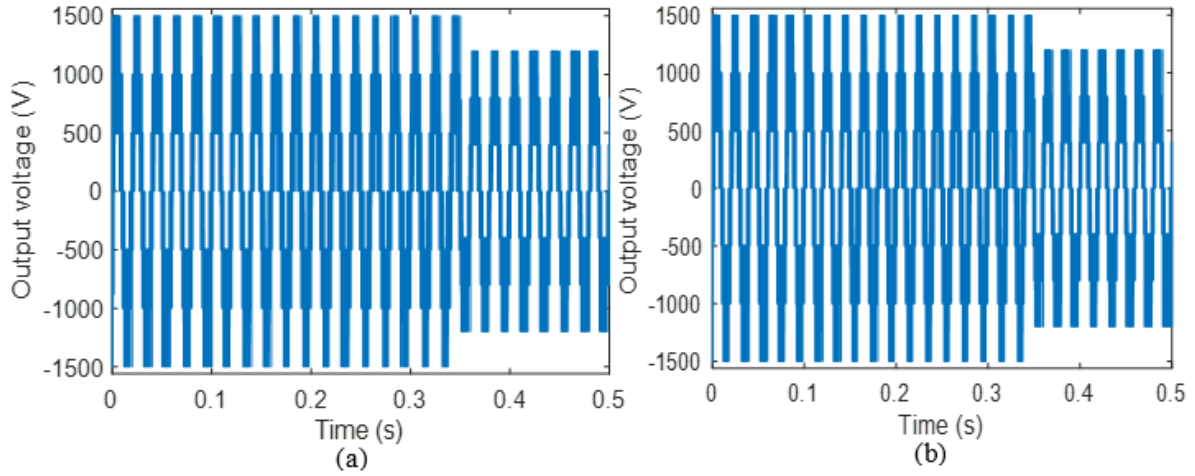

Figure 6. Evolution of output voltage (a: PI regulator, b: NN regulator)

The comparative study shows that both PI (Figure 5-a) and neural network (NN)-based regulators (Figure 5-b) achieve similar response times during startup. However, after disturbances at 0.35 s (300 V drop in input DC voltage, reducing E_{dc} from 1500 V to 1200 V), the nonlinear feedback decoupling strategy combined with NNs provides a much faster rebalancing of the floating capacitor voltages. For instance, the settling time of V_{C11} (stack 1) is reduced from 9.7 ms with PI to only 0.81 ms with the NN controller, representing a reduction of about 92%. Similar improvements are observed for the other capacitor voltages, with average reductions of nearly 79%. This faster stabilization ensures better voltage balancing, which directly translates into more symmetrical waveforms and enhanced output quality (Figure 6). This variation has no effect on the load current.

Load Current Regulation

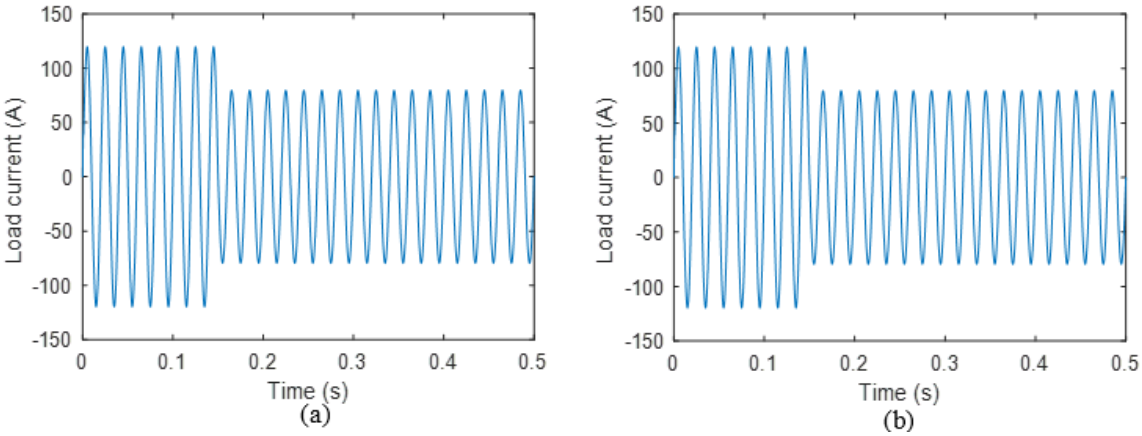

Figure 7. Evolution of load current (a: PI regulator, b: NN regulator)

When a variation in the load current is applied at 0.15 s (Figure 7) where we decrease the value of the reference load current from 120 A to 80 A, a reduction of 40 A, both PI and NN based regulators show similar overall performance, with only slight differences in dynamic response. The PI controller achieves satisfactory tracking with small overshoot and acceptable convergence time, while the NN-based regulator shows marginally faster stabilization and slightly reduced transient deviations. Thanks to the nonlinear feedback decoupling, capacitors voltages stability is maintained in both cases, although the NN regulator provides a minor improvement by further reducing the coupling effects between current dynamics and capacitor voltages. These results indicate that the two approaches perform comparably, with the NN-based method offering only incremental benefits.

Voltage-Current Decoupling

A key advantage of the nonlinear feedback decoupling framework is its ability to isolate voltage dynamics from current dynamics which is visible in figures 5, 6 and 7. In the PI-controlled inverter, a change in load current significantly perturbs the floating capacitor voltages, increasing rebalancing time and degrading output quality. In contrast, the NN-based controller preserves effective decoupling, allowing capacitor voltages to recover more quickly (57–92% faster depending on the cell), while maintaining stable and well-regulated current. This validates the capability of the proposed control to reduce cross-interactions between voltage and current, ensuring more predictable and stable performance.

Harmonic Distortion (THD)

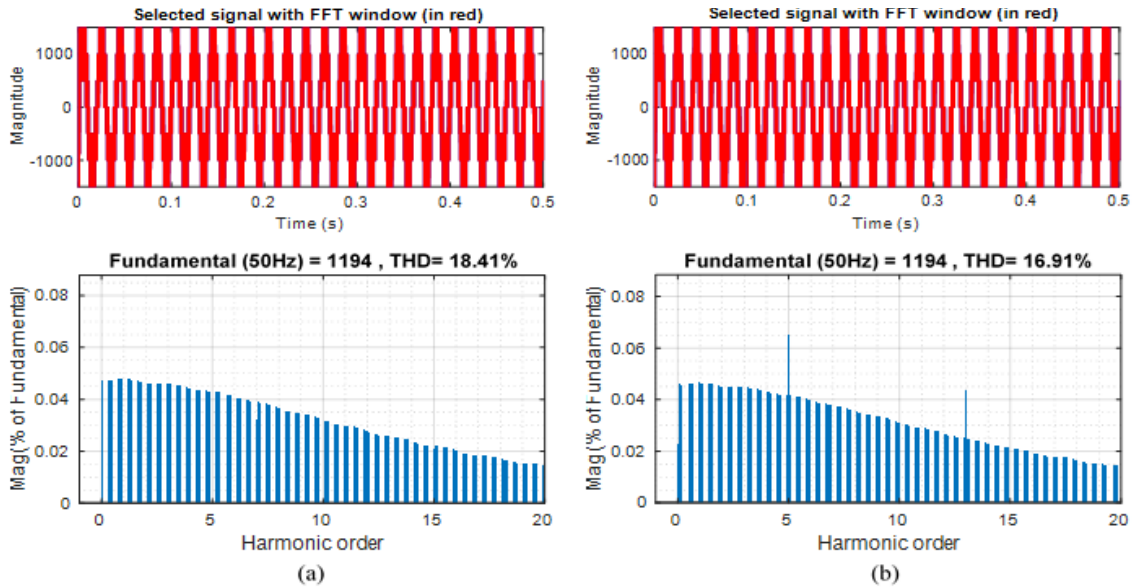

Figure 8. Output voltage with THD (a: PI regulator, b: NN regulator)

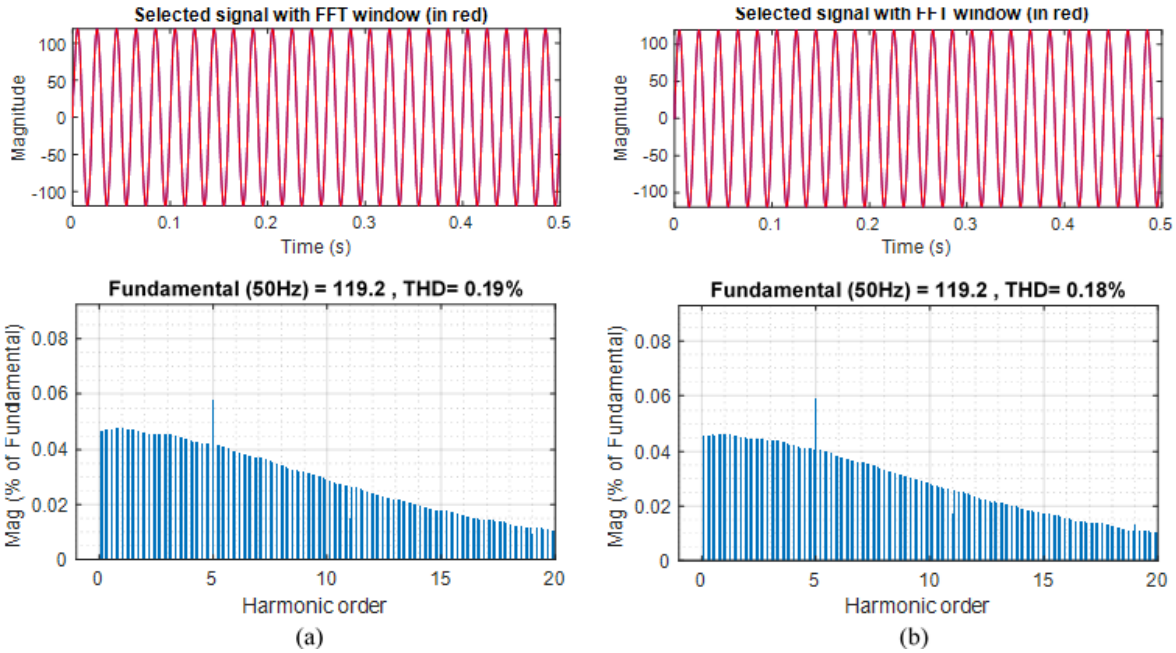

Figure 9. Load current with THD (a: PI regulator, b: NN regulator)

The NN-based approach provides a notable improvement in output waveform quality. The total harmonic distortion (THD) in the output voltage (figure 8) decreases from 18.41% with PI regulation to 16.91% with the NN controller, representing an 8.1% relative reduction. The current THD (figure 9) also decreases slightly, from 0.19% to 0.18%. Although the improvement in current quality is modest, the reduction in voltage THD is significant, as it reflects the improved voltage balancing achieved through faster capacitor regulation.

Overall Robustness

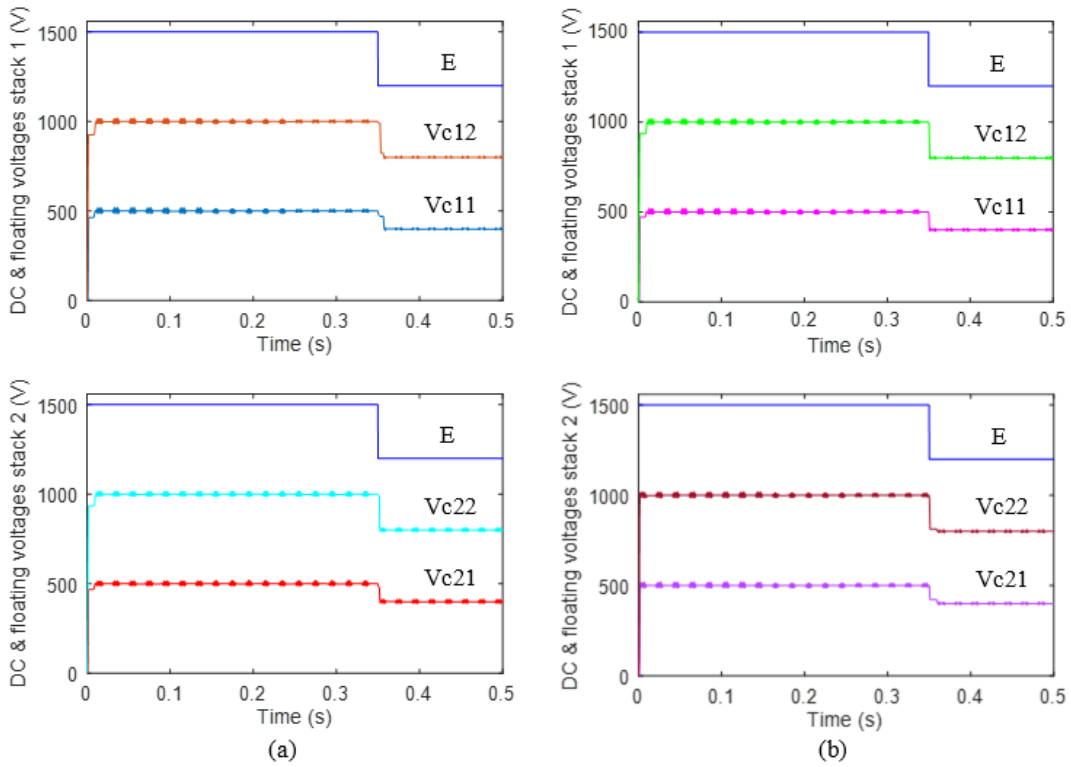

Figure 10. Evolution of DC input voltage and floating voltages _ robustness test (a: PI regulator, b: NN regulator)

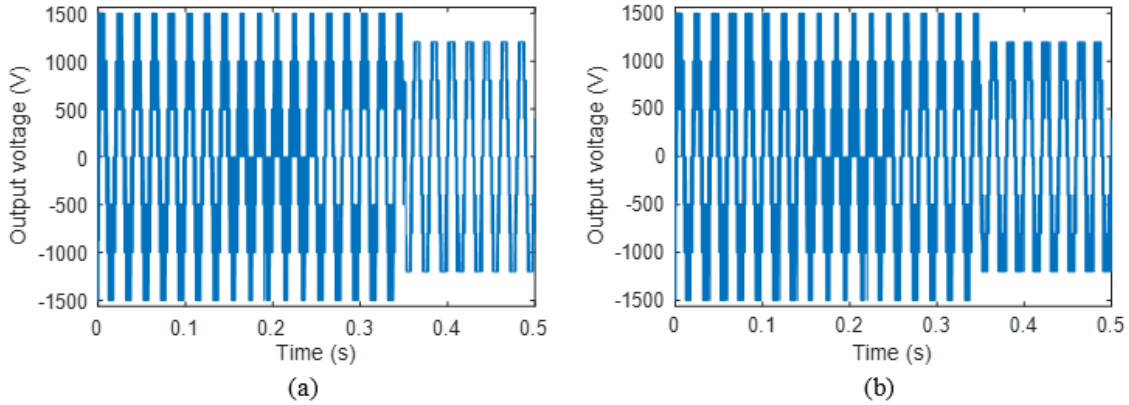

Figure 11. Output voltage _ robustness test (a: PI regulator, b: NN regulator)

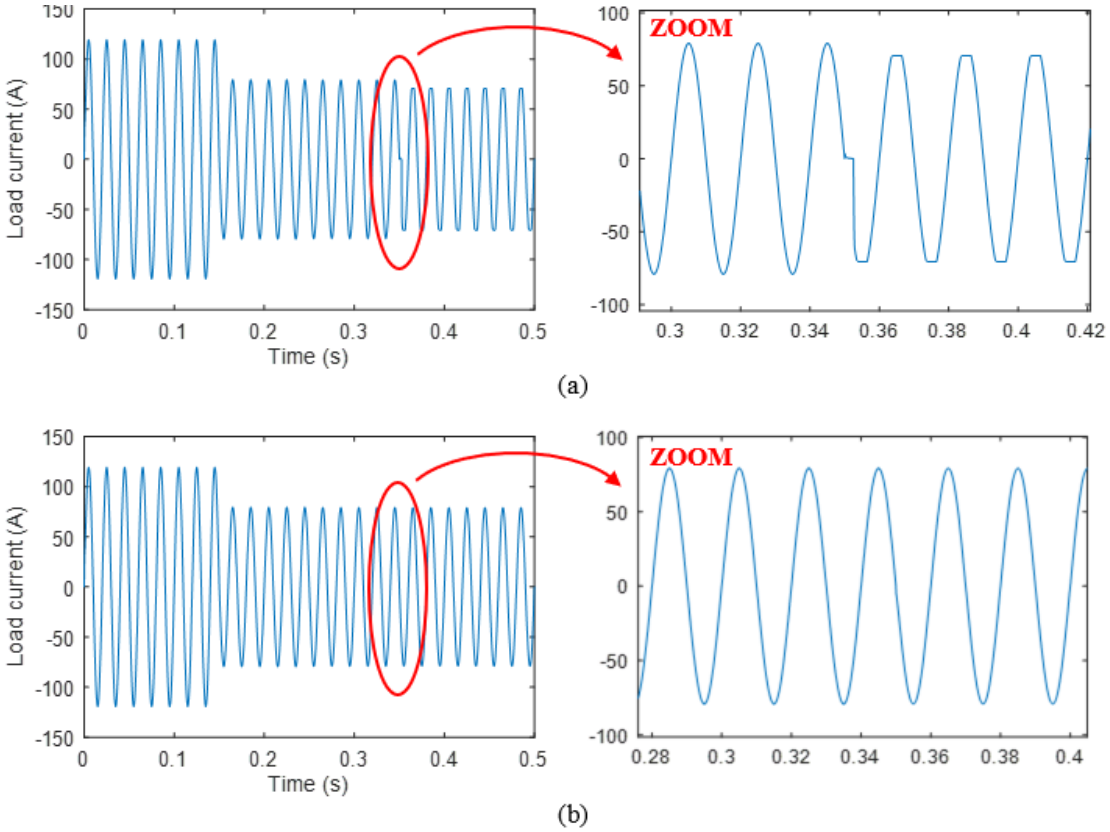

Figure 12. Load current _ robustness test (a: PI regulator, b: NN regulator)

Under different operating scenarios (figures 10, 11 and 12) -including, current steps (reduction of 40 A) at 0.15 s, load variations (50% increase in RL load) at 0.25 s and input DC voltage drops (drop in input DC voltage, reducing E_{dc} from 1500 V to 1200 V) at 0.35 s —the NN-based controller consistently maintains system stability, capacitor voltage balancing, and current regulation. In contrast, the PI-controlled system shows a lack of robustness, with degraded performance under the same disturbances. This superior robustness of the NN-based decoupling strategy can be attributed to the adaptive learning capability of neural networks, which enables real-time compensation of parameter uncertainties and external perturbations, while maintaining effective decoupling.

Summary

In summary, at equal system architecture and control objectives, the nonlinear feedback decoupling approach with NN-based regulators clearly outperforms the PI-controlled version. It ensures significantly faster capacitor voltage regulation (on average 79% faster after disturbances), more accurate load current tracking, reduced coupling between voltage and current dynamics, lower voltage THD, and superior robustness under parameter variations

and disturbances. These results confirm the effectiveness of the proposed method for achieving high-performance operation in stacked multicellular inverters.

Conclusion

This paper has introduced a novel control strategy for a 3×2 stacked multicellular inverter, combining nonlinear feedback decoupling with neural network-based regulation. Unlike conventional PI controllers, which are sensitive to parameter variations and load disturbances, the proposed approach leverages the adaptive capabilities of neural networks to approximate the nonlinear control law in real time and compensate for uncertainties. Simulation results in MATLAB/Simulink have confirmed that the method provides faster dynamic response, improved voltage regulation, and lower total harmonic distortion. These findings demonstrate the effectiveness of integrating nonlinear decoupling with intelligent control, establishing a robust and reliable solution for high-performance power conversion systems.

Scientific Ethics Declaration

* The authors declare that the scientific ethical and legal responsibility of this article published in EPSTEM journal belongs to the authors.

Conflict of Interest

* The authors declare that they have no conflicts of interest

Funding

* This research received no specific grant from any funding agency in the public, commercial, or not-for-profit sectors.

Acknowledgements or Notes

* This article was presented as a poster presentation at the International Conference on Technology, Engineering and Science (www.icontes.net) held in Antalya/Türkiye on November 12-15, 2025.

References

Aimé, M. (2003*). Evaluation et optimisation de la bande passante des convertisseurs statiques : Application aux nouvelles structures multicellulaire*. (Doctoral dissertation). National Polytechnic Institute of Toulouse, France.

Akagi, H. (2017). Multilevel converters: Fundamental circuits and systems. *Proceedings of the IEEE, 105*(11), 2048-2065.

Bakeer, A. I., Mohamed, S., Malidarreh, P. B., Hattabi I., & Liu, L. (2022). An artificial neural network-based model predictive control for three-phase flying capacitor multilevel inverter. *IEEE Access, 10*, 70305-70316.

Blaabjerg, F., & Ma, K. (2013). Future on power electronics for wind turbine systems. *IEEE J. Emerg. Sel. Topics Power Electron., 1*(3), 139-152.

Gateau, G. (1997). *Contribution à la commande des convertisseurs multicellulaires série* (Doctoral thesis). National Polytechnic Institute of Toulouse, France.

Gateau, G., Fadel, M., Bensaid, R., & Meynard, T. A. (2002). Multicells converters: Active control and observation of flying-capacitor voltages. *IEEE Transactions on Industrial Electronics*, *49*(5), 998-1008.

Gateau, G., Maussion, P., & Meynard, T. A. (1997). De la modélisation à la commande non linéaire des convertisseurs multicellulaires série. Application à la fonction hacheur. *J. Phys III France*, *7*(6), 1277-1305.

Hanafi, S., Fellah, M. K., Achar, A., Yaichi, M., Djeriri, Y., Benbouhenni, H., Colak, I., Benkhoris, M. F., & Wira, P. (2025). Enhancing space vector modulation control in parallel multicellular converters using artificial neural networks. *Electrical Engineering, 107*, 13529-13545

Hanafi, S., Fellah, M. K., Djeriri, Y., & Benkhoris, M. F. (2021). Control of parallel multicellular DC/AC converter including monolithic inter-cell transformer in a real-time environment. *Revue Roumaine des Sciences Techniques - Série Électrotechnique et Énergétique, 66*(3), 169-174.

Hanafi, S., Fellah, M. K., Yaichi, M., & Benkhoris, M. F. (2014). Nonlinear feedback decoupling control applied to stacked multicellular converter. *Revue Roumaine des Sciences Techniques – Série Électrotechnique et Énergétique, 59*(1), 97-106, 2014.

Hanafi, S., Fellah, M. K., Yaichi, M., & Benkhoris, M. F. (2016). Control of stacked multicellular inverter. *Revue Roumaine des Sciences Techniques – Série Électrotechnique et Énergétique, 61*(3), 278-282.

Haykin, S. (2009). *Neural networks and learning machines* (3rd ed.). Upper Saddle River, NJ: Pearson.

Isidori, A. (1995). *Nonlinear control systems* (3rd ed.). London: Springer.

Jiang, H., Chen, Y., & Kang, Y. (2021). application of neural network controller and policy gradient reinforcement learning on modular multilevel converter (mmc) - a proof of concept. *2021 IEEE 4th International Electrical and Energy Conference (CIEEC)*, Wuhan, China, 1-6,

Kouro, S., Malinowski, M., & Rodriguez, J. (2010). Multilevel power converters. *IEEE Trans. Ind. Electron., 57*(8), 2553-2580.

Lienhardt, A. M., Gateau, G., & Meynard, T. A. (2005). Stacked multicell converter (SMC): Reconstruction of flying capacitor voltages. *In Proceedings of the 31st Annual Conference of the IEEE Industrial Electronics Society* (*IECON 2005*) (pp. 1–6). IEEE.

Meynard, T. A., Foch, H., Thomas, P., Courault, J., Jakob, R., & Nahrstaedt, M. (2002). Multicellular converters: Basic concepts and industry applications. *IEEE Trans. Ind. Electron., 49*(5), 955-964.

Peña-Alzola, R., Liserre, M., Blaabjerg, F., Sebastián, R., Dannehl, J., & Fuchs, F. W. (2014). Systematic design of the lead–lag network method for active damping in lcl-filter-based three-phase converters. *IEEE Transactions on Industrial Informatics, 10*(1), 43-52.

Rivera, M., Yaramasu, V., Llor, A., Rodriguez, J., Wu, B., & Fadel, M. (2012). Digital predictive current control of a three-phase four-leg inverter. IEEE Transactions on Industrial Electronics, 60(11), 4903-4912.

Rodriguez, J., Franquelo, L. G., Kouro, S., León, J. I., Portillo, R. C., & Martin Prats, M. Á. (2009). Multilevel converters: An enabling technology for high-power applications. *Proceedings of the IEEE, 97*(11), 1786–1817.

Wu, B. (2006). *High-power converters and ac drives.* Hoboken, NJ: Wiley-IEEE Press.

Author(s) Information

Salah Hanafi
Djillali Liabes University of Sidi Bel-Abbes.
ICEPS Laboratory, Sidi Bel-Abbes, Algeria.
Contact e-mail : *salah.hanafi@univ-sba.dz*

Mohammed Karim Fellah
Djillali Liabes University of Sidi Bel-Abbes.
ICEPS Laboratory, Sidi Bel-Abbes, Algeria.

Youcef Djeriri
Djillali Liabes University of Sidi Bel-Abbes.
ICEPS Laboratory, Sidi Bel-Abbes, Algeria.

Mohamed Fouad Benkhoris
University of Nantes.
IREENA Laboratory, Saint-Nazaire, France.

Abdelhakim Saim
University of Nantes.
IREENA Laboratory, Saint-Nazaire, France.

Djamel Ziane
University of Nantes.
IREENA Laboratory, Saint-Nazaire, France.

Patrice Wira
University of Haute Alsace.
MIPS Laboratory, Mulhouse, France.

To cite this article:

Hanafi, S., Fellah, M. K., Djeriri, Y., Benkhoris, M. F., Saim, A., Ziane, D., & Wira, P. (2025). Robust nonlinear control of a 3×2 stacked multicellular inverter using neural network-based regulation. *The Eurasia Proceedings of Science, Technology, Engineering and Mathematics (EPSTEM), 38*, 56-68.